Eur. Phys. J. D **28**, 361–366 (2004)
DOI: 10.1140/epjd/e2003-00318-y

THE EUROPEAN PHYSICAL JOURNAL D

Relaxation of photoexcited Na_3F

J.M. L'Hermite[a], V. Blanchet, A. Le Padellec, B. Lamory, and P. Labastie

Lab. Collisions Agrégats Réactivité, UMR 5589 du CNRS, IRSAMC-UPS, 118 route de Narbonne, 31062 Toulouse, France

Received 28 July 2003 / Received in final form 31 October 2003
Published online 6 January 2004 –

Abstract. This paper describes the spectroscopy of Na_3F both in the frequency and time domains. The photoionization efficiency curve shows two thresholds, associated to two isomers. The excited electronic states of the C_{2v} isomer have been probed by photodepletion spectroscopy, and the results are used to analyze a time-resolved study of photoexcited Na_3F, probed by photoionization. The pump-probe signal clearly shows damped oscillations, the period of which is fitted to 390 ± 10 fs, close to twice the previously measured bending mode of Na_2F [1], while the relaxation time is 1275 ± 50 fs.

PACS. 36.40.Qv Stability and fragmentation of clusters – 33.50.-j Fluorescence and phosphorescence; radiationless transitions, quenching (intersystem crossing, internal conversion)

1 Introduction

Small Na_nF_{n-p} clusters can be considered as formed of n Na^+ ions and $(n-p)$ F^- ions, which tend to form a rock-salt lattice, together with p excess electrons, which are to be accommodated in the structure. It is easy to understand that the electronic arrangement, and hence the ionization potential, is highly structure dependent, which has indeed been verified in references [2–9]. In this respect, it may happen that different isomers of the same cluster present a significant difference between their ionization potential. This strong correlation between the structure and the ionization potential allows to monitor selectively the passage through one specific isomer in time-resolved experiments. Indeed, the ionization probability may become time-dependent, provided the probe pulse energy is low enough to photoionize only one isomer while the molecule is excited in such a way that it wanders through several structures. Na_3F is such a cluster, with two isomers, which have a vertical ionization energy that differs by almost 0.5 eV. The lowest isomer is a quasi-planar C_{2v} structure (deformed rhombic structure with the F atom on the short side of an elongated Na_3 triangle) with a vertical ionization energy of roughly 4.9 eV, while the second lowest isomer is a 3D C_{3v} structure (pyramid with the F atom capping an equilateral Na_3 triangle). This second isomer lies slightly higher in energy (∼65 meV above) and has a vertical ionization energy of 4.4 eV [4,5]. The ground state of the ion is linear and the adiabatic ionization potential is 4.26 eV [10]. These structures as well as the energetics of the system are depicted in Figure 1. Such a large difference in vertical ionization energies makes this cluster an ideal system to test the above ideas.

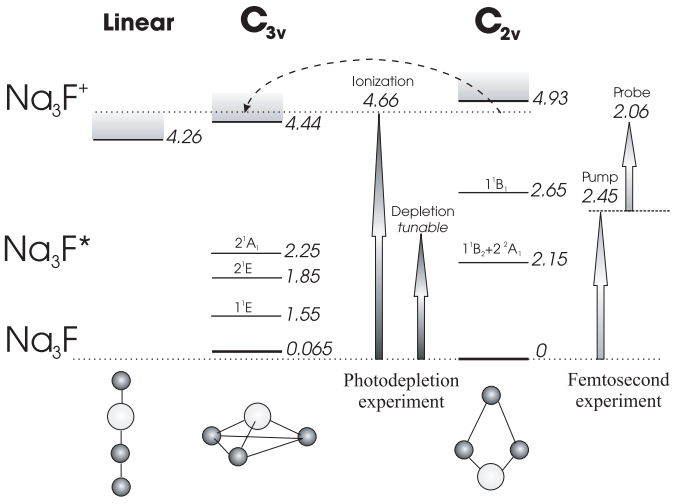

Fig. 1. Energetic of Na_3F (the drawing is not to scale). The energies (in italic) are in electron Volts. The two lowest isomers of Na_3F and the lowest isomer of Na_3F^+ are shown. The dashed arrow from C_{2v} to C_{3v} indicates a possible preionization scheme in the one-photon photoionization experiment (see text Sect. 2.2).

Recently, a femtosecond pump-probe experiment on Na_2F has been reported [1]. A periodic bending motion was identified, with a period of roughly 200 fs. The C_{2v} isomer of Na_3F is electronically very close to Na_2F+Na. If a bending motion is initiated in the Na_2F part, the F atom may come close to the third Na atom, then come back to the initial position, and so on. If the oscillation motion is similar to that of Na_2F, the position of closest distance

[a] e-mail: J-M.Lhermite@irsamc.ups-tlse.fr

between F and the third Na will be attained every other oscillation, which means that the period is expected to be roughly twice that of Na_2F.

The present paper is divided into three parts: the first part describes experiments performed in the nanosecond regime to determine the ionization potential and the absorption spectra. The second part accounts for the femtosecond pump-probe experiment and in the third part, a discussion is opened that deals with the relaxation dynamics in this cluster and the phenomenological model used to fit the various time constants.

2 Spectroscopy in the nanosecond regime

2.1 Experimental set-up

The apparatus has been already described in reference [7]. The clusters are produced by laser vaporization (doubled Nd:YAG laser at a wavelength of 532 nm) of a sodium rod, with helium at about 5 bars as a carrier gas. The repetition rate can be varied from 2.5 Hz to 10 Hz. The carrier gas contains a small amount (about 1%) of SF_6, which provides the fluorine atoms. In this configuration, the vibrational temperature of the formed clusters is roughly 400 K [11]. Based on the 65 meV difference between both isomers of Na_3F, the populations are expected to be roughly 85% of C_{2v} geometry and 15% of C_{3v} for a Boltzmann distribution. The ionizing laser beams are focused onto the cluster beam between the first two plates of an axial Wiley Mac-Laren Time-Of-Flight mass spectrometer (TOFMS) with a reflectron. The mass resolution of this device is about $m/\Delta m = 4000$. The clusters are detected on a tandem of micro-channel plates and averaged by a high-speed digital oscilloscope (Lecroy).

In order to determine the photoionization efficiency curve, the clusters are ionized by the second harmonic of the signal output of an Optical Parametric Oscillator (OPO) which has been tuned from 230 nm to 325 nm. The laser bandwidth is roughly 1 cm^{-1} and the typical fluence is 10^5 W/cm^2 at the interaction volume.

In a second experiment, the photofragmentation yield is determined by photodepleting the ground state with a visible pulse (OPO signal output, 5×10^5 W/cm^2) and probing 200 ns later (typically) the remaining population with the fourth harmonic of a Nd:YAG laser at 266 nm (2×10^6 W/cm^2). The absorption cross-section is obtained by comparing the ion yields with and without the visible pulse.

2.2 Photoionization efficiency curve

The photoionization efficiency curve is displayed in Figure 2. The ionization threshold is close to the 4.4 eV calculated one for the C_{3v} isomer [5]. The experimental photoionization efficiency increases from threshold up to a first maximum at 4.65 eV and then decreases sharply. Such a decrease of the ion yield when the laser energy exceeds the ionization potential has already been observed in sodium fluoride clusters, in particular for Na_nF_{n-3} [12]. It is interpreted as a fragmentation induced by the excess energy. However, the signal does not drop as sharply in general. At 4.9 eV, a kind of second threshold appears, in good agreement with the ab initio vertical ionization potential of the C_{2v} isomer [5]. From this second threshold, the signal increases once again up to a second maximum reached at about 5.0 eV and then decreases. The second maximum is lower than the first one. At first glance, it is surprising: according to the hypothesis of a Boltzmann distribution of population, we should have more C_{2v} than C_{3v} isomers. However, first, it is well-known that in molecular beams the relative population of isomers is ruled not only by their relative energy but also by entropic and nucleation considerations. Second, since for several isomers the IP is lower than 4.65 eV, indirect photoionization might occur through some resonant preionization path (see Fig. 1): once excited at 4.65 eV, the C_{2v} cluster might evolve toward such an isomer and then be ionized. This intense peak could indeed reflect an autoionizing state of this isomer, rather than an exceptional ionization yield of the C_{3v} geometry. It is hard to conclude at this stage however, and we defer further discussion to the next paragraph.

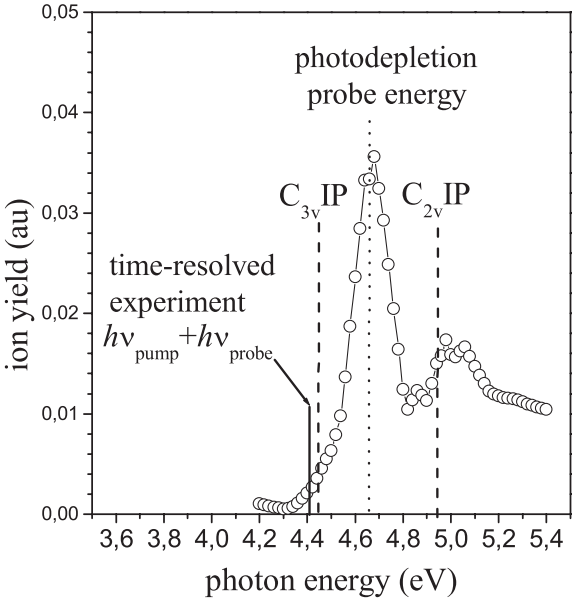

Fig. 2. Photoionization efficiency curve of Na_3F. Ab initio vertical ionization energies of the two isomers are indicated by vertical dashed lines. The UV probe energy used in the photodepletion experiment and the femtosecond pump + probe total energy are also shown.

2.3 Photodepletion experiment

Prior to the photodepletion experiment, a resonant-two photon ionization analysis was carried out. No signal was observed. Previous experiments on Na_nF_{n-3} clusters revealed the same feature [12]. It seems likely that every excited state in the visible range is a short lived state,

Table 1. Excited states expected from ab initio calculations [5] and the ones observed through the photodepletion experiment.

C_{2v}			C_{3v}		
states	ab initio	experiment	states	ab initio	experiment
$1^1B_2 + 2^1A_1$	2.15 eV	2.18 eV	1^1E	1.55 eV	-
1^1B_1	2.65 eV	2.5 eV	2^1E	1.85 eV	-
			2^1A_1	2.25 eV	-
1^2A_1 – ion	4.93 eV	∼4.8 eV	1^2A_1 – ion	4.44 eV	∼4.4 eV

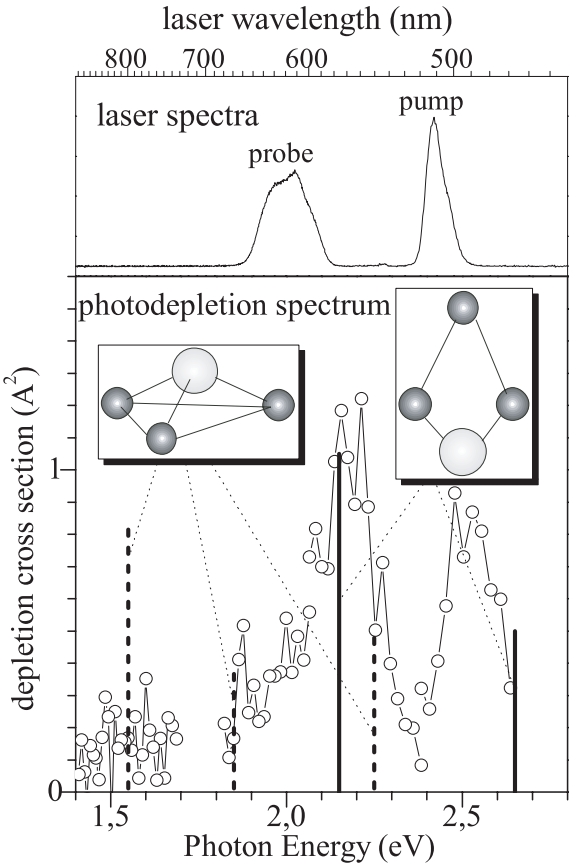

Fig. 3. Photoabsorption spectrum of Na_3F as determined by photodepletion spectroscopy (circles). The calculated oscillator strengths for vertical excitations are indicated for both the C_{2v} and C_{3v} structures by solid lines and dashed lines respectively [5]. The spectra of the two femtosecond pulses used in the time-resolved experiment are also plotted.

whatever the Na_3F isomer. This last point motivates the time-resolved studies described further. The photodepletion yield is displayed in Figure 3. Note that the probe at 266 nm photoionizes directly into the sharp peak observed in Figure 2, which means that we monitor whatever isomer associated with this peak. The calculated oscillator strengths for vertical electronic excitations [5] are indicated in Figure 3 for both the C_{2v} and C_{3v} isomers. The main band in the photodepletion spectrum lies around 2.2 eV, in good agreement with the quasi-degenerated excited states 1^1B_2, 2^1A_1 of the C_{2v} structure. The second band observed at about 2.5 eV is attributed to an excitation in the 1^1B_1 state of the same isomer, although it is slightly shifted to the red. Preliminary calculations by Durand et al. [10] show that indeed the absorption frequency is red-shifted for this transition when thermal excitations are considered.

Moreover, if the photodepletion experiment were sensitive to the C_{3v} isomer, a significant absorption band would have appeared around 1.5 eV. The spectrum does not show any evidence of a band at this energy. The suggestion arising out of this photodepletion experiment is that the observed spectrum is due to the C_{2v} isomer. We cannot rule out the presence of the C_{3v} isomer in the beam however, since its photoionization yield at 266 nm could be very low in comparison with that of the C_{2v} structure. Despite this possibility, we consider as initial species only the C_{2v} isomer. Table 1 summarizes for each isomer the excited states and ionization potentials determined by ab initio calculations [5] and the ones observed through the photodepletion and the photoionization experiments.

3 Time resolved spectroscopy

3.1 Excitation scheme

In order to study nuclear and relaxation dynamics in a pump-probe scheme, a number of constraints are to be fulfilled. Ideally, the pump has to be resonant with a ground state excitation, while the probe should not. Moreover, since we detect the ion signal, the total pump + probe energy should be just above the C_{3v} vertical ionization potential (4.4 eV), where the signal is likely to be most sensitive to any change in the geometry.

In order to simplify the dynamics, the vibrational energy in the excited state should be taken as low as possible, which lead us to choose the pump energy for instance in the rising edge of the first band (∼2.0 eV) or either the second band (∼2.4 eV) in Figure 3. By selecting these two wavelength ranges, we reach as well the ionization threshold at 4.4 eV. Thus, we were performing two pump-probe experiments with this excitation scheme: pump at 2.0 eV, probe at 2.4 eV and vice versa.

3.2 Experimental set-up

Each laser pulse is generated by a Non-collinear Optical Parametric Amplifier (NOPA) [13]. The input of these devices is taken from the output of a 1 kHz–1 mJ chirped

pulse amplification (CPA) laser centered at 800 nm. One NOPA generates a 15 nm-broadband pulse centered at 510 nm (2.4 eV, the NOPA lower wavelength limit) compressed with Brewster-cut fused silica prisms. The second NOPA generates a 40 nm-broadband pulse centered at 620 nm (2.0 eV) compressed with chirped mirrors (50 fs^2/reflection). These pulses are combined with a beam splitter. The cross-correlation signal, taking into account all the dispersive media on the beams path, and recorded through a 20 μm-thick BBO crystal, has a full-width at half maximum of 180 ± 10 fs by assuming a Gaussian shape (Figs. 5–6). It allows to determine the time delay $\Delta t = 0$ of the pump-probe signal. The linear chirps estimated from this cross-correlation measurement are both in the range of $\phi'' = 800$ fs^2. Several studies have already pointed out the influence of a small linear chirp on the pump pulse relative to ultrafast dynamics [14–16]. A linear chirp on the pump might affect significantly the amplitude of the pump-probe oscillations by focusing or not the wavepacket, depending on the potential energy surface curvatures [14,15]. As long as the time-resolution is high enough, this effect does not change the frequency component of the wavepacket. Therefore no alteration of the time dependence is expected [16]. Nevertheless, for larger chirps and especially when the pump spectrum involves several absorption bands, the pump frequency sweeping has to be considered [17]. In the present experiment however, there is only one band involved in the excitation and the chirp is expected to be less than 1×10^3 fs^2. The main consequence of a chirp on the pump pulse is therefore to reduce the time-resolution. A chirp of the probe pulse has also been investigated on simple system via time-resolved photoelectron spectroscopy, showing a connection between the chirp parameter and the width of the photoelectron spectrum [18–20]. Nonetheless the time dependency of the ionization is not affected by such a chirp. By recording the ion signal even at the ionization threshold, the main consequence of a chirp on the probe pulse is again to reduce the time resolution.

The pump and probe pulses are focused via the same 500 mm-lens onto the cluster beam. The position of this lens is adjusted such that the background signal due to multiphoton ionization by either pulse alone is minimal. Since ionization with the 2.4 eV light requires 2 photons, whilst 2.0 eV requires 3 photons, we had to decrease the intensity at 2.4 eV, respective to the other. The best configuration was obtained with the focus at 3 cm behind the cluster beam and the intensities of the 2.4 eV and the 2.0 eV pulses at 2.5 GW/cm^2 and 20 GW/cm^2 respectively. Note that the laser pulse to pulse stability is better than 85%.

The poor pulse to pulse stability of the cluster beam is the main source of fluctuations of the ion signal. First, in order to reduce the noise, we measured the surface of the Na_3F peak rather than the intensity of the maximum. Second, averaging over several shots allows overcoming partially this problem. However, the long term fluctuations (depending mainly on the part of the sodium rod that is vaporized) are not eliminated by the averaging. In order to get rid of spurious temporal variations, we took advantage of the non-zero ion signal obtained with the 2.4 eV pulse alone. This signal can reasonably be considered as proportional to the number of Na_3F clusters in the beam. To normalize the pump-probe ion yield with respect to the native population of Na_3F, we proceeded as follows: the ion signal is recorded alternatively with (S^{on}) and without (S^{off}) the 2 eV laser. Let us call a step i the recording of both signal S_i^{on} and S_i^{off}. For each pump-probe delay Δt, 100 steps are recorded. The relative ion yield for each delay Δt is the ratio of the averaged values $\langle S^{on}_{i=1..100}\rangle / \langle S^{off}_{i=1..100}\rangle$.

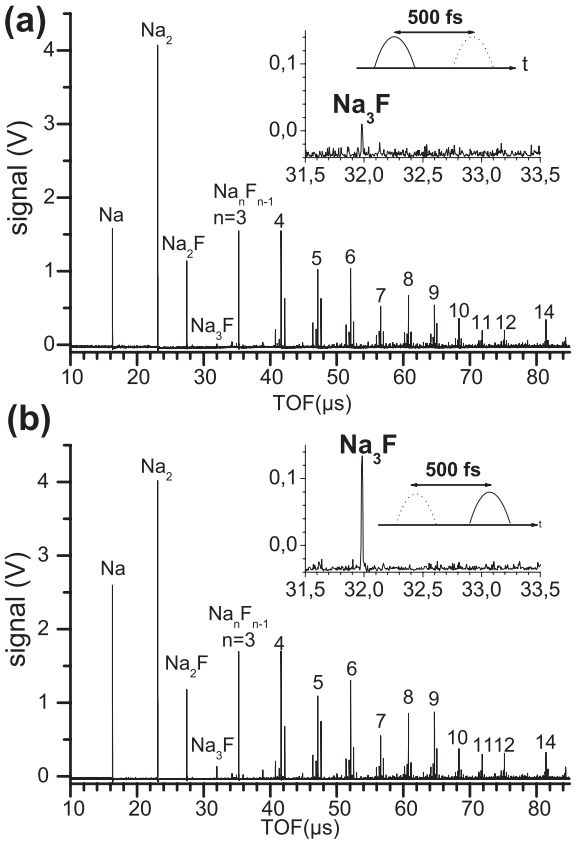

Fig. 4. Mass spectra obtained with femtosecond lasers ionization. The numbers above some of the peaks refer to n in the main series Na_nF_{n-1}. Two different time configurations are considered: (a) the 2.4 eV laser pulse (dotted line) arrives 500 fs after the 2.0 eV pulse (full line). (b) The 2.0 eV laser pulse arrives 500 fs after the 2.4 eV pulse. The signal of Na_3F is the only one that changes significantly from one spectrum to the other (the vertical scale is the same on the two expanded views).

3.3 Result and fitting procedure

Figure 4 shows two mass spectra averaged over 200 laser shots, with respectively positive and negative time delay between the two femtosecond pulses. Note first that a large number of clusters are ionized, with an intensity that is rather independent on the delay. Only Na_3F displays a marked dependence on the time delay. The intensity is

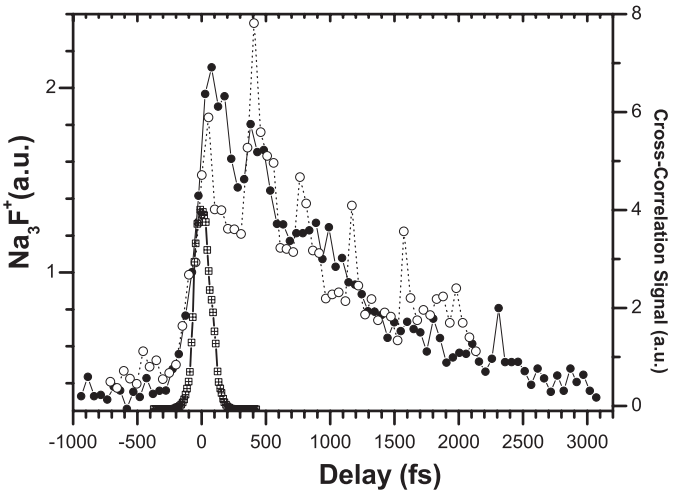

Fig. 5. Na_3F^+ pump-probe signals (circle symbols) and cross-correlation trace (crossed square symbols). The two pump-probe signals shown are recorded for the same pump pulse but a slightly different probe pulse: 2.04 eV (empty circles) and 2.08 eV (filled circles).

much larger when the 2.4 eV pulse is sent before the 2.0 eV one (inset (a) of Fig. 4). A more careful study indicates that for the delay of Figure 4b, the Na_3F^+ intensity is the sum of the intensities obtained with each of the lasers sent separately. Thus, from now on, we will refer to the 2.4 eV pulse as the pump and the other as the probe, and the delay will be considered as positive when the 2.4 eV pulse arrives before the 2.0 eV pulse.

Typical pump-probe signals are shown in Figure 5. The sum of the energies of the two lasers is 4.44 eV, at the threshold of vertical ionization from the ground electronic state of the C_{3v} isomer. It is not enough to ionize the C_{2v} isomer in a vertical excitation scheme. This restricts the geometries that can be photoionized from the excited state by the probe pulse. The cross-correlation curve gives the experimental $\Delta t = 0$ time delay. For positive delay, the signal shows an oscillatory behavior together with an exponential decay. We have slightly tuned the probe energy from 2.04 eV up to 2.08 eV. The main features as the decay remain, except that the amplitude of the oscillations decreases when the energy increases. These oscillations might be related to vibrational dynamics and the ability to observe them is fixed mainly by the strong geometry restriction on the ionization probability. The investigation as a function of the excitation energy is mainly limited by the wavelength range of the beam splitter ($\lambda_{probe} > 570$ nm). The study as a function of the pump energy is confined by the range of emission from the NOPA.

In order to extract the typical time constants of the wavepacket dynamics, the pump-probe signal is modeled by

$$S(\tau) = |g_{cc}(t) \otimes f(t)|^2 \tag{1}$$

where $g_{cc}(t)$ is linked to the cross-correlation signal with a FWHM $\tau_{cc} = 180$ fs by:

$$g_{cc}(t) = e^{-2(\ln 2)(t/\tau_{cc})^2} \tag{2}$$

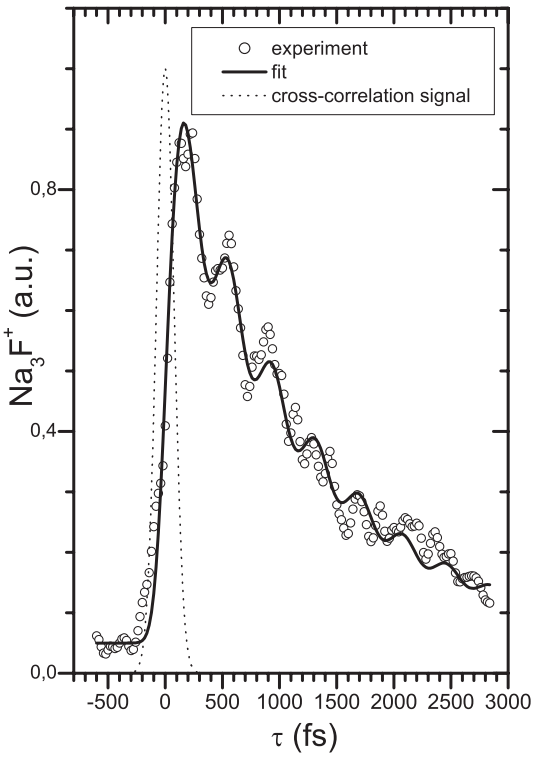

Fig. 6. Fit (solid line) of the pump-probe signal (empty circle symbols) using equations (1–3) with a cross-correlation signal of 180 fs FWHM (dotted line). The experimental signal is averaged over 5 recordings.

$f(t)$ models the population in the excited state that might be photoionized. In order to reproduce the main features observed in Figure 5, $f(t)$ is a decaying function with an oscillating part:

$$f(t) = e^{-t/2\tau_e}\left(e^{i\Omega t} + \alpha e^{-i(\Omega t - \varphi)}\right) \tag{3}$$

where the pure decay part is homogeneous and characterized by τ_e, the period of the oscillations is 2Ω, α fixes the amplitude of the oscillations, and φ allows to introduce a shift T_s on the first maximum relative to the origin.

Five time-resolved records are averaged to give the experimental data of the Figure 6. Theoretical curves using equations (1–3) are adjusted by least square fitting using a conjugate gradient method. The cross-correlation time is fixed to $\tau_{cc} = 180$ fs. The best fit parameters τ_e, Ω, φ and α slightly vary as a function of the initial values used in the non-linear fitting procedure. Thus, we performed a set of fits using random initial values. Statistics over these fits leads to $\tau_e = 1275 \pm 50$ fs, $\pi/\Omega = 390 \pm 10$ fs, $\varphi = 3.47 \pm 0.50$ rad, $\alpha = 4.6 \times 10^{-2} \pm 2 \times 10^{-4}$. This results in a time-shift $T_s = 180 \pm 30$ fs. The result of this fit is shown in Figure 6.

4 Discussion

This fit is just to assess the typical values of relaxation dynamics in Na_3F. It has several limitations that need to

be mentioned. First, as confirmed by wavepackets calculations currently in progress, the value of φ is very difficult to interpret; that is why its value is not discussed into details. This will be discussed in a forthcoming paper. Second, the chirp of the two pulses is only taken into account via the cross-correlation time-width. However, the pump-probe signal seems robust in its time structure from day to day, despite the fact that the chirp might fluctuate.

The evolution of the ion signal as a function of the pump-probe delay shows two main features, namely an oscillatory behavior and a damping. The oscillations may be interpreted as a variation of the ionization potential induced by nuclear motion, or a vibrational excitation in the excited state populated by the pump laser pulse. These oscillations as well as the overall time-dependent pump-probe signal vanish with a decay time of about 1 ps. This damping results from a drop of the Na_3F population open to ionization. Two alternative explanations may be given: either, the population of Na_3F^* decreases due to fragmentation (calculations show that at least one fragmentation channel is opened when Na_3F is excited at 2.4 eV: $Na_3F^* \rightarrow Na_2F + Na$ [10]) or Na_3F^* evolves toward configurations in which it is no longer ionized. Ideally, the fragmentation hypothesis could be monitored through an increase of the Na_2F signal in the mass spectrum. Unfortunately, the background signal of Na_2F is large which makes such a tiny variation undistinguishable. A time-resolved photoelectron spectroscopy, as already suggested for Na_2F, might allow to better characterize the process. Wavepacket dynamics calculations are also performed to get a better insight [21].

Another surprising result from this time-resolved experiment is the absence of a clear time-dependency for negative delay. Indeed as mentioned above (see Fig. 3), the 620 nm pulse might also excite the first band, further photoionized by the 510 nm pulse. However, there is a slight disagreement between the experimental data and the fit in the first -200 fs. As a matter of fact, the experimental curve has a small "bump" in this region that may be due to a "probe-pump" scheme with a very small decay time. More investigations are necessary at that stage to confirm it. A main explanation to the absence of visible signature at negative delay, may be easily explained by the strong requirement imposed on the ionization. Indeed, ionizing at threshold limits the number of geometries that might be probed.

5 Conclusion

We have presented the energy spectrum of Na_3F investigated by both photodepletion experiment and one-photon ionization. Based on this spectroscopy, we have studied the relaxation dynamics via time-resolved experiment. Oscillations superposed on a 1 ps decay characterize the pump-probe signal. This is analyzed as a manifestation of vibrational dynamics undergoing IVR, photoisomerisation or either dissociation. More investigations, such as time-resolved photoelectron spectroscopy or time-resolved photofragment ionization are needed to experimentally underpin the present analysis. Moreover this dynamics might now be assessed via quantum wavepacket propagation on potential energy surfaces calculated using two-electron pseudopotential Hamiltonian [21].

We thank B. Chatel for technical support on NOPA and G. Durand and F. Spiegelman for providing vertical and adiabatic transition energies prior to publication. Discussions with M.C. Heitz and C. Meier about Na_3F vibrational relaxation are gratefully acknowledged.

References

1. S. Vajda, C. Lupulescu, A. Merli, F. Budzyn, L. Wöste, M. Hartmann, J. Pittner, V. Bonačić-Koutecký, Phys. Rev. Lett. **89**, 213404 (2002)
2. E.C. Honea, M.L. Homer, P. Labastie, R.L. Whetten, Phys. Rev. Lett. **63**, 394 (1989); E.C. Honea, M.L. Homer, R.L. Whetten, Phys. Rev. B **47**, 7480 (1993)
3. G. Rajagopal, R. Barnett, A. Nitzan, U. Landmann, E.C. Honea, P. Labastie, M.L. Homer, R.L. Whetten, Phys. Rev. Lett. **64**, 2933 (1990)
4. V. Bonačić-Koutecký, J. Pittner, J. Koutecký, Chem. Phys. **210**, 313 (1996)
5. V. Bonačić-Koutecký, J. Pittner, Chem. Phys. **225**, 173 (1997)
6. J. Giraud-Girard, D. Maynau, Z. Phys. D **23**, 91 (1992); J. Giraud-Girard, D. Maynau, Z. Phys. D **32**, 249 (1994)
7. P. Labastie, J.-M. L'Hermite, P. Poncharal, M. Sence, J. Chem. Phys. **103**, 6362 (1995)
8. P. Poncharal, J.-M. L'Hermite, P. Labastie, Z. Phys. D **40**, 10 (1997)
9. G. Durand, F. Spiegelmann, P. Poncharal, P. Labastie, J.-M. L'Hermite, M. Sence, J. Chem. Phys. **110**, 7884 (1999)
10. G. Durand, M.C. Heitz, F. Spiegelmann, private communication (2003)
11. P. Labastie, J.-M L'Hermite, P. Poncharal, L. Rakotoarisoa, M. Sence, Z. Phys. D **34**, 135 (1995)
12. P. Labastie, J.-M. L'Hermite, P. Poncharal, Z. Phys. Chem. **203**, 15 (1998)
13. G. Cerullo, M. Nisoli, S. De Silvestri, Appl. Phys. Lett. **71**, 3616 (1997)
14. C.J. Bardeen, Q. Wang, C.V. Shank, Phys. Rev. Lett. **75**, 3410 (1995)
15. T. Saito, T. Kobayashi, J. Phys. Chem. **106**, 9436 (2002)
16. M.-C. Yoon, D. H. Jeong, S. Cho, D. Kim, H. Rhee, T. Joo, J. Chem. Phys. **118**, 164 (2003)
17. S. Zamith, V. Blanchet, B. Girard, J. Andersson, S. Sorensen, I. Hjelte, O. Björneholm, D. Gauyacq, J. Norin, J. Mauritson, A. L'huillier, J. Chem. Phys. **119**, 3763 (2003)
18. A. Assion, M. Geisler, J. Helbing, V. Seyfried, T. Baumert, Phys. Rev. A **54**, R4605 (1996)
19. S. Meyer, C. Meier, V. Engel, J. Chem. Phys. **108**, 7631 (1998)
20. L. Nugent-Glandorf, M. Scheer, D.A. Samuels, A.M. Mulhisen, E.R. Grant, X. Yang, V.M. Bierbaum, S.R. Leone, Phys. Rev. Lett. **87**, 193002 (2001)
21. M.-C. Heitz, G. Durand, F. Spiegelman, C. Meier, J. Chem. Phys. **118**, 1282 (2003)